

# Detection of paramagnetic excited states in noble-gas cryocrystals by ESR

R. A. Zhitnikov, Yu. A. Dmitriev, and M. E. Kaimakov

*A. F. Ioffe Physicotechnical Institute, Academy of Sciences of the USSR*

(Submitted 28 November 1990)

*Zh. Eksp. Teor. Fiz.* **99**, 1804–1815 (June 1991)

Short-lived paramagnetic centers have been detected in cryocrystals of the noble gases Ne, Ar, Kr, and Xe, formed by condensation of these gases on a cold substrate together with the products of the gas discharge taking place in them. These centers were recorded by ESR in cryocrystals of the pure rare gases directly in the course of the condensation. An explanation is given for the nature of the centers observed, which are manifested as metastable excited  $^3P_2$  atoms of these elements, which are trapped in the FCC cryocrystal of the noble gas and which distort and rearrange their immediate vicinity in the cryocrystal and are subjected to the action of the anisotropic electric field of this environment.

## 1. INTRODUCTION

Publications dealing with matrix isolation in frozen rare gases and with ESR studies of such systems have thus far referred to stabilized impurity atoms and ions in the ground states only.<sup>1</sup>

Our work<sup>2-5</sup> developed an improved technique and apparatus for stabilizing in frozen gases the products of a gas discharge and for studying them by means of the ESR method. This made it possible to obtain a number of new results and to observe new quantum effects for the H, D, and N atoms, stabilized in matrices of H<sub>2</sub>, D<sub>2</sub>, N<sub>2</sub>, Ne, and Ar.<sup>2-5</sup>

In this technique, the sample is obtained directly in the cavity of the ESR spectrometer. This makes it possible to observe and study by means of the ESR method the actual process of formation of the sample with the matrix-isolated products of the gas discharge, and also to detect and study in this sample the short-lived paramagnetic centers associated with the products of the gas discharge.

In the present work, this technique has made it possible to observe, apparently for the first time, short-lived paramagnetic centers in noble-gas cryogenic crystals by means of the ESR method. These centers constitute local excited states in noble-gas cryocrystals.

The experimental technique and the experimental results obtained and their possible explanation are briefly described below.

## 2. EXPERIMENTAL TECHNIQUE

The technique used here differs from the familiar ones in the following characteristics. The solid state samples studied are obtained by condensation of gas flows on the thin-walled bottom of a liquid-helium-filled quartz test tube, this bottom being located at the center of the cavity of the ESR spectrometer. The gas discharge and the additional condensable matrix gas are cooled with liquid nitrogen, and the products of an RF gas discharge without intermediate feeding tubes are aimed in a vacuum directly onto the substrate, i.e., onto the bottom of the quartz test tube, so that any possible loss of the products of the discharge on the walls of the feeding tubes is precluded.

The experimental apparatus includes a 3-cm ESR spectrometer with a cavity cooled by liquid nitrogen, a helium cryostat, a low-temperature gas-discharge unit, a system for injecting and purifying the gases, an RF generator for

exciting an electrodeless gas discharge, measuring instruments, and means of evacuation.

Figure 1 shows the cavity of the ESR microwave spectrometer with a low-temperature gas-discharge unit and a substrate cooled by liquid helium, on which the sample to be studied is condensed.

Here 1 is the cylindrical resonator of the 3-cm ESR spectrometer, which is attached to the flange 3 by means of the indium gasket 2. This flange is sealed to the vacuum housing 4 of a helium cryostat. The bottom 5 of the liquid-helium-filled quartz test tube 6 is the low-temperature substrate for the gases being condensed. To improve the removal of the heat of condensation, the bottom is made as thin as possible, 0.3–0.5 mm; 7 is the waveguide section. An electrodeless RF gas discharge is triggered in the glass tube 8; 9 is an outlet 0.5–0.7 mm in diameter. The magnetic-field modulation current of the ESR spectrometer with a frequency of 100 kHz is fed to the modulation pins 10 through molybdenum wires 11 sealed into the glass. Four pins inserted into the cavity form two loops of modulating current. The described glass part of the structure is sealed to the copper can 12, which in turn is sealed to the cover of the cavity 13. This cover is fastened to the cavity by means of the indium gasket 14. The entire construction shown in Fig. 1 is immersed in a liquid-nitrogen bath. An RF (14-MHz) generator is used to maintain the discharge. The RF power is fed through a coaxial cable to the coil 15, wound over the discharge tube 8. The generator operates in both the pulsed and continuous modes. The pulse width can be decreased to 10  $\mu$ sec, and the maximum pulse repetition rate is 30 kHz. The glass tube 16 serves to measure the gas pressure in the cavity.

The experimental procedure consists in the following. The noble gas, precooled to 77 K, is passed through the liquid-nitrogen-cooled discharge tube 8, in which is excited an electrodeless pulsed RF discharge with a pulse width  $\tau = 30 \mu$ sec and a pulse repetition rate of 1 kHz. Through the aperture 9 in the diaphragm of the tube 8, particles of this gas together with the gas-discharge products pass into the evacuated cavity 1 and reach the bottom 5 of the test tube 6, filled with liquid helium at 1.2–4.2 K. During condensation of the gas into the cryocrystal with the gas-discharge products trapped in the latter, continuous recording of the ESR of these samples, which condense on the substrate 5 at the center of the cavity, is performed. The time constant of the sec-

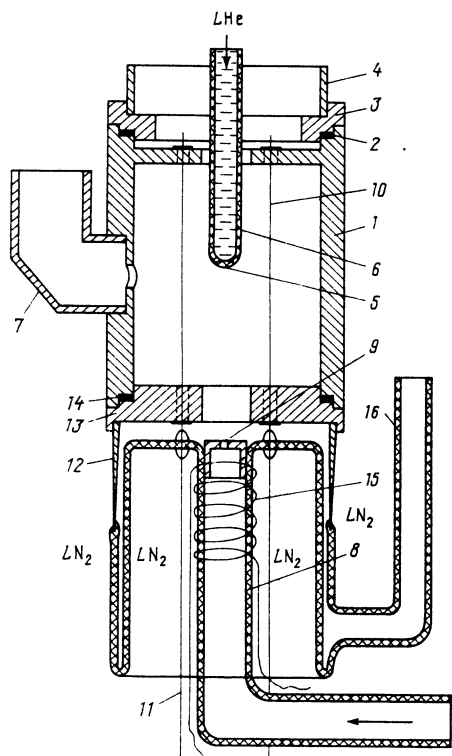


FIG. 1. Diagram of the main component of an experimental apparatus with the cavity of an ESR spectrometer, a gas-discharge unit, and a liquid-helium-cooled quartz finger, on the bottom of which the sample studied is condensed (for notation, see text).

tion recording the ESR spectra is 0.1 sec, the rise rate of the magnetic field is 0.2 gauss/sec, and the magnetic-field modulation frequency is 100 kHz.

The short-lived centers are separated from the stable ones by switching off the gas discharge in the tube 8, i.e., switching off the RF voltage on the coil 15 during the recording of the ESR spectrum.

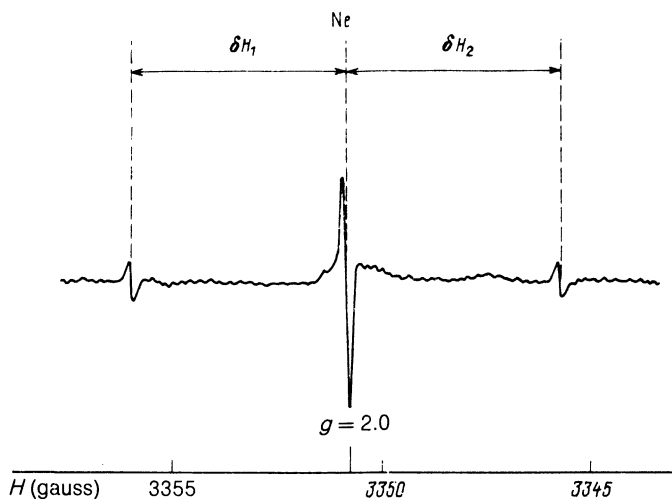


FIG. 2. ESR spectrum of short-lived paramagnetic centers in the neon cryocrystal. Substrate temperature  $T = 1.4$  K, gas flow through the discharge  $Q = 3$  mmole/h, resonance frequency  $f_{res} = 9379.31$  MHz.

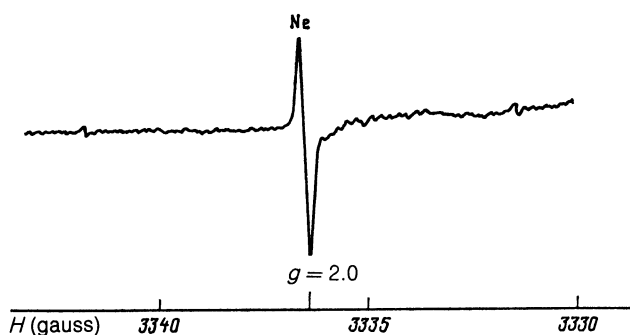


FIG. 3. ESR spectrum of short-lived paramagnetic centers in the neon cryocrystal with a different line-strength ratio;  $T = 4.2$  K,  $Q = 3$  mmole/h,  $f_{res} = 9339.00$  MHz.

We used high-purity noble gases with the following impurity content: in Ne, 0.004%, in Ar, 0.007%, in Kr, 0.0009%, and in Xe, 0.0003%. Thus the impurity concentrations were sufficiently small to exclude their influence on the experimental results.

### 3. EXPERIMENTAL RESULTS

#### (a) Neon and Argon

Experiments involving the trapping of gas-discharge products in cryocrystals of pure neon and argon and aimed at finding short-lived paramagnetic centers during the condensation gave the ESR spectra shown in Figs. 2–6. In these experiments, pure argon or neon was passed through the liquid-nitrogen-cooled gas-discharge tube 8, then condensed on the substrate 5 together with the products of the discharge. These spectra (Figs. 2–6) were observed only during a continuous flow, onto the cold ( $T = 1.2$ – $4.2$  K) substrate 5, of neon or argon from the tube 8 along with the products of the gas discharge taking place in this tube. When the gas

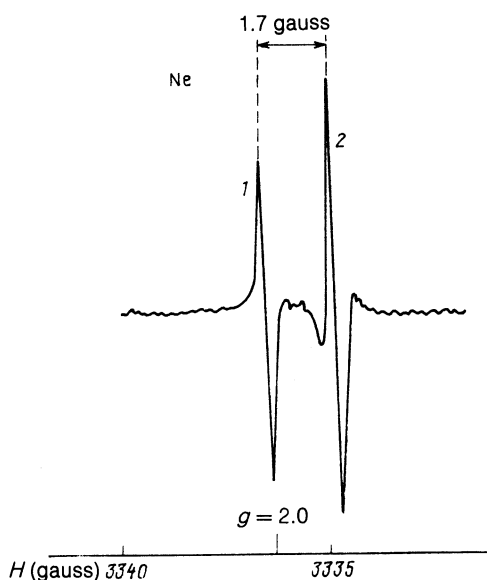


FIG. 4. ESR spectrum of short-lived paramagnetic centers in the neon cryocrystal with increased gas flow through the discharge;  $T = 4.2$  K,  $Q = 7$  mmole/h,  $f_{res} = 9338.94$  MHz.

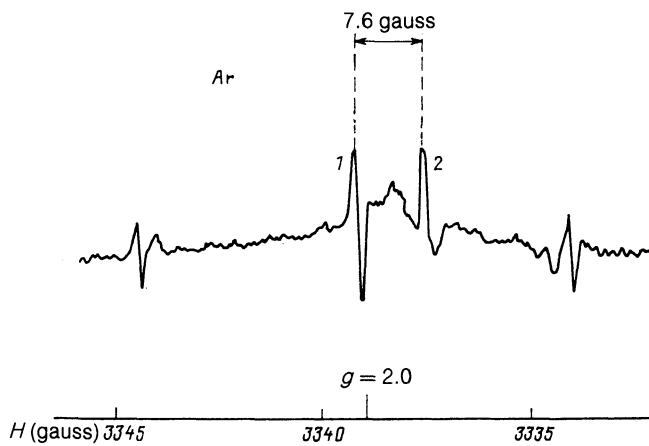


FIG. 5. ESR spectrum of short-lived paramagnetic centers in the argon cryocrystal with increased gas flow through the discharge;  $T = 4.2$  K,  $Q = 22$  mmole/h,  $f_{\text{res}} = 9346.60$  MHz.

discharge was switched off, the ESR signal disappeared immediately, and the ESR spectrum record was cut off. Thus, the paramagnetic centers responsible for these spectra have short lifetimes. According to estimates based on the time constant of the section recording the spectra, the lifetime of these centers is  $\leq 0.1$  sec.

It was found that these paramagnetic centers are localized in frozen neon or argon. Thus, when the gas discharge is



FIG. 6. ESR spectrum of short-lived paramagnetic centers in the neon cryocrystal with changes in the satellite lines;  $T = 4.2$  K,  $Q = 4$  mmole/h,  $f_{\text{res}} = 9437.39$  MHz.

switched on in the tube 8 and in the presence of a neon or argon flow from this tube into the cavity, but in the absence of liquid helium in the test tube 6, i.e., when no cryocrystals are formed, the ESR signals indicated above are completely absent. This indicates that the observed short-lived paramagnetic centers are located in the neon or argon cryocrystals, not in the gaseous phase. This is also confirmed by an examination of the properties of these centers, which are discussed below.

The ESR spectra, obtained at comparatively small gas flows through the gas discharge zone ( $\leq 5$  mmole/h), were found, for cryocrystals of pure neon and argon, to be completely identical both in appearance (i.e., as in Figs. 2 and 3) and in all quantitative characteristics. Nor were any differences observed between the spectra obtained at the substrate temperatures  $T = 1.2$  and  $4.2$  K.

The parameters of these spectra, which agree completely within the measurement error with those for the neon and argon cryocrystals, are shown in Table I. Here the  $g$  factor pertains to the center line, which is the strongest. The remaining notation is clear from Fig. 2.

The relative strengths of the center and satellite lines in the spectra shown in Figs. 2 and 3 changes from experiment to experiment, and in neon and argon, from the maximum strength of the satellite lines to their complete disappearance. As an example, Figs. 2 and 3 show spectra with different relative strengths of the center and satellite lines. The variability of the relative strength of the center line and the doublet of satellite lines indicates that this doublet and the center line belong to different paramagnetic centers.

As the gas flow through the discharge tube increases, and when it exceeds 7 mmole/h, new lines appear in the spectra of the short-lived centers in the neon and argon cryocrystals. The lines shown in Figs. 2 and 3 are preserved. Figure 4 gives the ESR spectrum for neon for an increased gas flow. Two closely spaced lines are seen, with line 1 coinciding with the center line in Figs. 2 and 3 and having a  $g$  factor equal to that given in Table I. The spacing between these lines amounts to 1.7 gauss. Figure 5 shows the ESR spectrum for argon also for an increased gas flow. Here line 1 coincides with the center line in Figs. 2 and 3, and the new line is separated from it by 1.6 gauss. Thus, as the gas flow grows, the same changes may occur in the ESR spectra of short-lived centers for neon and argon, as follows from the similarity of the spectra in Figs. 4 and 5. In some experiments, however, for the same gas flow as in Fig. 5, two more lines appeared between the two center lines shown in this figure, and all four lines had comparable strengths.

An interesting change during the growth of the gas flow was observed in the satellite lines of the spectrum in some experiments. Figure 6 shows such a spectrum for neon. It is obvious that the simple doublet spectrum of Figs. 2 and 3 has assumed a characteristic structure in Fig. 6.

#### (b) Krypton and Xenon

The experiments with Kr and Xe differed somewhat from those with Ne and Ar. Because the freezing point is higher than in Ne and Ar, the experiments with Kr and Xe had to be performed with the gas discharge at room temperature without liquid-nitrogen cooling of the gas-discharge tube 8 or of the gas supplied to it. The cavity was also at room temperature, and this intensified the boiling of helium in the

TABLE I. Parameters of ESR spectra of short-lived centers in neon and argon cryocrystals.

Noble gas	Number of iments	T, K	g Factor	$\delta H_1$ (gauss)	$\delta H_2$ (gauss)	Width of center line $\Delta H_1$ (gauss)	Width of satellite lines $\Delta H_2$ (gauss)
Ne	7	4,2	1,99987 (12)	5,19(8)	5,24(8)	0,1-0,2	0,1-0,2
Ar	4	4,2	1,99986 (12)	5,21(8)	5,18(8)	0,1-0,2	0,1-0,2

test tube 6 and shortened the time of the experiment. Otherwise, the experimental technique was the same as in the case of Ne and Ar. In the Kr and Xe cryocrystals, ESR spectra of short-lived paramagnetic centers were also observed. However, these spectra were different from those observed in Ne and Ar, although they were equally short-lived, i.e., disappeared immediately when the discharge was switched off.

Figure 7 shows the ESR spectrum of the short-lived centers in the krypton cryocrystals. Two lines with g factors indicated in Table II are present in the spectrum. Neither line coincides completely with the center line of the spectra of Figs. 2 and 3.

Figure 8 shows one of the ESR spectra of short-lived centers in Xe cryocrystals. This spectrum consists of several close lines of different strengths and is distinguished by poor reproducibility. From one experiment to the next, the number, location, and strength of the lines change, but they all are close to one another within the confines of the spectrum of Fig. 8, are located around  $g = 2.0$ , and have a short lifetime, i.e., the entire spectrum disappears immediately when the gas discharge is switched off.

#### 4. INTERPRETATION OF THE RESULTS

To elucidate the nature of the observed short-lived paramagnetic centers, it is necessary to consider the products of the discharge in the rare gas that may enter the cryocrystal of this gas being condensed, as well as the possible action of the gas discharge on the cryocrystal already frozen onto the substrate, and to compare the results of this examination with the properties and characteristics of the ESR spectra shown in Figs. 2-8 and in Tables I and II.

In order to reach the cold substrate 5 on which the sample is condensed, the gas-discharge products must travel a distance  $\sim 3$  cm through vacuum. If they are noble-gas atoms their thermal velocities are of order  $10^4$  cm/sec, i.e.,

only particles with a lifetime  $\geq 10^{-4}$  sec can reach the substrate. The only neutral products of the discharge in the noble gas which satisfy this condition are excited metastable atoms of this gas in the lower  $^3P_2$  and  $^3P_0$  states (for free  $^3P_2^0$  atoms, the lifetimes have the values<sup>6</sup>  $\tau(\text{Ne}) = 20$  sec,  $\tau(\text{Ar}) = 60$  sec,  $\tau(\text{Kr}) = 85$  sec,  $\tau(\text{Xe}) = 150$  sec, and for  $^3P_0^0$  atoms, the lifetimes range from 400 sec for neon to 0.08 sec for xenon). The entry of charged particles, i.e., electrons and ions, from the gas discharge into a growing cryocrystal of rare gas, as well as bombardment by these particles of the cryocrystal already formed, is impossible, since observation of the ESR spectra of short-lived centers is carried out as the cryocrystal condenses. Therefore, the strong magnetic field of the ESR spectrometer  $H_0 = 3300$  gauss is switched on all the time; it is transverse to the flow of these charged particles, deflects them to one side, and prevents them from reaching the substrate 5, i.e., the sample. Thus, for 1-keV electrons in a 3300-gauss magnetic field, the orbit radius is 0.32 mm.

Finally, the solid cryocrystal of noble gas already formed on the substrate, as well as the gas being condensed, can both be subjected to irradiation by light from the gas discharge, including VUV. The action of the light from the discharge in the noble gas on the cryocrystal of this gas or gas at the instant of condensation can be produced only by the short-lived  $^3P_1$  and  $^1P_1$  atoms. These excited atoms cannot cause the formation of the observed ESR spectra, since the radiative lifetimes of the  $^3P_1$  and  $^1P_1$  atoms are too short: for all noble gases, they are of order  $10^{-8}$ - $10^{-9}$  sec. Such lifetimes are associated with ESR linewidths  $\geq 5$ -50 gauss, whereas the observed spectra have linewidths of the order of

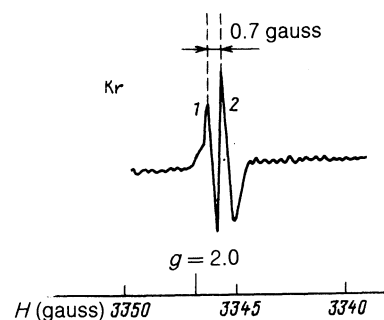


FIG. 7. ESR spectrum of short-lived paramagnetic centers in the krypton cryocrystal;  $T = 4.2$  K,  $Q = 5$  mmole/h,  $f_{\text{res}} = 9368.63$  MHz.

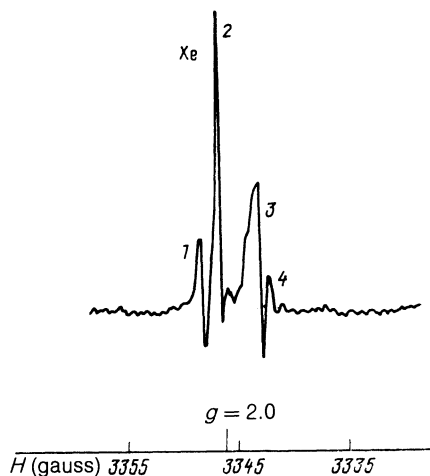


FIG. 8. ESR spectrum of short-lived paramagnetic centers in the xenon cryocrystal;  $T = 4.2$  K,  $Q = 6$  mmole/h,  $f_{\text{res}} = 9366.92$  MHz.

TABLE II. Parameters of ESR spectra of short-lived centers in krypton and xenon cryocrystals.

Noble gas	Number of experiments	T, K	g Factors of lines				Linewidths (gauss)			
			$g_1$	$g_2$	$g_3$	$g_4$	$\Delta H_1$	$\Delta H_2$	$\Delta H_3$	$\Delta H_4$
Kr	2	4,2	2,00056 (12)	2,00095 (12)	—	—	0,23 (5)	0,23 (5)	—	—
Xe*	4	4,2	1,9987	1,9997	2,0020	2,0026	0,5	0,4	0,5	0,7

For spectrum in Fig. 8.

0.1 gauss (see Tables I and II and Figs. 2–8); this requires a lifetime of the paramagnetic center on the order of  $5 \times 10^{-7}$  sec. At the same time, it is known that the lifetime, for example, of the  $^3P_2$  atoms of neon in a cryocrystal of this gas is  $\geq 6 \times 10^{-4}$  sec.<sup>7</sup> For cryocrystals of the other noble gases, the lifetime of  $^3P_2$  atoms is most probably also  $> 10^{-6}$  sec. Therefore, paramagnetic centers based on  $^3P_2$  atoms of noble gases trapped in cryocrystals should satisfy the requirement of a fairly small ESR linewidth, consistent with that observed experimentally. However, these  $^3P_2$  atoms, like  $^3P_0$  atoms, cannot for all practical purposes be formed under action of radiation from the gas discharge, since the radiative transitions  $^1S_0 \rightarrow ^3P_2, ^3P_0$  to these metastable states from the ground state  $^1S_0$  are forbidden. Hence, the radiative radiation of the gas discharge cannot be responsible for the formation of the paramagnetic centers producing the observed ESR spectra.

Thus, the observed centers (Figs. 2–8) can only be due to the entry into the rare gas cryocrystal of atoms of this gas in the  $^3P_2$  state directly from the gas discharge. Atoms in the  $^3P_0$  state, which can also reach the crystal from the discharge, should be excluded from consideration, since they are diamagnetic and cannot form paramagnetic centers in the cryocrystal.

Thus, the cause of the formation of the observed short-lived paramagnetic centers is the trapping, in the growing rare-gas cryocrystal, of atoms of this gas in the metastable  $^3P_2$  state. This atom is paramagnetic and, as was noted

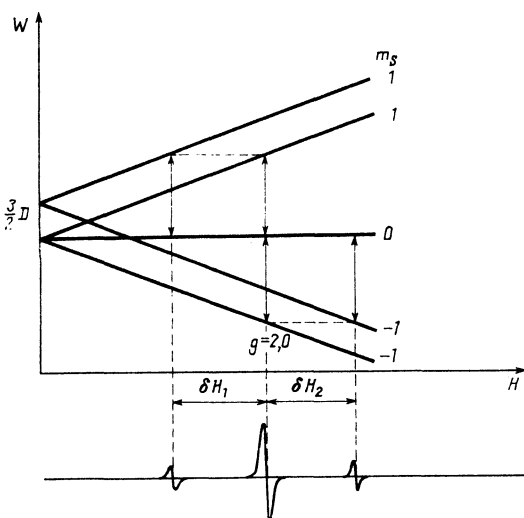


FIG. 9. Splitting of the levels of an atom with spin  $S = 1$  in an axial electric crystal field and appearance of satellite lines in the ESR spectrum.

above, can have a sufficiently long lifetime in the cryocrystal to provide for the experimentally observed small ESR linewidth,  $\Delta H_{1,2} \sim 10^{-1}$  gauss.

However, a significant difficulty arises here. This is because in the observed ESR spectra (Figs. 2–8), all the lines have  $g$  factors that are very close to  $g = 2.0$ , whereas the  $^3P_2$  state has a  $g$  factor of 1.5, and its lines should be at entirely different magnetic fields (i.e., for  $g = 2.0$ ,  $H_{res} = 3300$  gauss, as is the case experimentally, and for  $g = 1.5$ ,  $H_{res} = 4400$  gauss). It was found experimentally that in magnetic fields close to 4400 gauss, the ESR spectra are completely absent. The following explanation is possible here. Apparently, the  $^3P_2$  rare-gas atom in the cryocrystal of this gas is stabilized so that the crystal electric field acting on it has a low (for example, tetragonal) symmetry. In such a field, the  $^3P$  term splits into two levels with  $m_L = \pm 1$  and 0.<sup>8</sup> If this splitting is sufficiently large, then at helium temperature (4.2–1.2 K), practically only the lower level with  $m_L = 0$  will be populated, for which the  $g$  factor is  $g = 2.0$ . These atoms, which constitute the majority of trapped  $^3P_2$  atoms, probably give the intense center line with  $g = 1.9999$  in the spectra of Ne in Figs. 2 and 3 and in the spectra of Ar (see Table I).

The spectrum consisting of the two satellite lines in Figs. 2 and 3 can be explained as follows. If the atom in the  $^3P_2$  state is localized at a crystal site where the crystal field acting on it has axial symmetry, then the state with  $m_L = 0$  in the zero magnetic state will split into two levels with  $m_S = \pm 1$  and 0.<sup>8</sup> For this case, the levels of the atom in the magnetic field and the ESR transitions are shown in Fig. 9. From this figure, taking the values for  $\delta H_1 = \delta H_2 = \delta H_{1,2} = 5.2$  gauss from Table I, one can determine the splitting of the  $^3D$  levels  $m_S = \pm 1$  and 0 in a zero magnetic field:  $^3D = \delta H_{1,2} g \beta / h = 2.8 \times 10^6 \delta H_{1,2}$  Hz = 14.6 MHz. The fraction of  $^3P_2$  atoms trapped at sites with such a crystal field is apparently small and may change from one experiment to the next, and this accounts for the variability of the strength of the satellite lines in Figs. 2–3.

It can be assumed that the majority of the  $^3P_2$  noble-gas atoms are trapped in the substitution positions of a face-centered cubic (FCC) noble-gas crystal and give an intense center line in the ESR spectrum in Figs. 2 and 3, and a smaller fraction of  $^3P_2$  atoms are trapped in the octahedral interstitial site of this crystal and give satellite lines. The fraction of the latter atoms may obviously change from one experiment to the next, depending on uncontrollable variations in experimental conditions.

Note that in an undistorted FCC crystal, these trapping sites have a crystal electric field of very high (cubic) symmetry, so that splitting of the  $^3P$  state cannot result. A low-

symmetry (anisotropic) crystal field causing the observed ESR spectra of  ${}^3P_2$  atoms with  $g = 2.0$  apparently arises because of distortion of the lattice of the noble-gas cryocrystal by the outer  $s$  shell of this  $np^5(n+1)s$   ${}^3P_2$  atom. Distortion of the FCC lattice of the crystal by the noble-gas  $P$  atom present in this lattice and the local rearrangement of this lattice are discussed in Ref. 9. It is shown that in this case, separation of the nearest atoms of the lattice may cause additional atoms of this lattice to penetrate into the immediate vicinity of the  $P$  atom and to disturb the cubic symmetry of this environment,<sup>9</sup> i.e., produce a local electric field of low symmetry acting on the  ${}^3P_2$  atom.

It is also indicated in Ref. 9 that the process of distortion of the lattice by the  $P$  atom may proceed through metastable intermediate variants of the configurations of the immediate neighborhood with certain delays in these configurations. Each of these configurations of the immediate neighborhood should be associated with a different symmetry of the crystal electric field acting on the  ${}^3P_2$  atom. This may account for the appearance, as the experimental conditions change, of new lines in the ESR spectra for neon and argon in Figs. 4–6, as well as the presence of two or more lines in the ESR spectra for krypton and xenon in Figs. 7 and 8. This is how Ref. 9 explains the splitting of the  $P$  levels in these cryocrystals, observed earlier in experiments on the cathodoluminescence of cryocrystals of noble gases.<sup>10,11</sup> In our experiments, an increase in the gas flow of Ne or Ar to the substrate may result in heating of the sample, growth of the size of its crystallites, and appearance of trapped  ${}^3P_2$  atoms for which the process of distortion of the immediate vicinity now takes place far from the surface of the sample, in the interior of the crystals and at a higher temperature. This may cause a change in the conditions of local rearrangement of the lattice around certain groups of  ${}^3P_2$  atoms<sup>11</sup> and gives rise to the additional lines in the spectra of Figs. 4, 5, and 6.

The explanation of the origin of the ESR spectra of short-lived paramagnetic centers (Figs. 2–8) also involved a discussion of the possibility of their relationship to excimer molecules of noble gases, which could have been manifested in the noble-gas cryocrystal by forming during its condensation according to the reaction  $R({}^3P_2) + R({}^1S_0) \rightarrow R_2^*({}^3\Sigma_u^+)$ . However, such an explanation of the observed ESR spectra of short-lived centers is highly improbable for the following reasons. First of all, the reaction of formation of excimer molecule  $R_2^*({}^3\Sigma_u^+)$  itself has a very low probability in both the gas phase (triple collisions are necessary) and the cryocrystal, where the time of formation of such a molecule, at least in neon, is much longer than the lifetime of a single  ${}^3P_2$  atom in the cryocrystal relative to the radiation.<sup>7,9–11</sup>

In addition, practically all the excimer molecules  $R_2^*$  of noble gases have zero nuclear spin. It follows from the properties of symmetry of the  ${}^3\Sigma_u^+$  state of a diatomic homonuclear molecule with zero nuclear spin that the rotational quantum numbers for such a molecule can only be odd,<sup>12</sup> i.e.,  $N = 1, 3, 5$ , etc. In the case of odd  $N$ , the  $g$  factor of such a molecule  $\leq 1$ , whereas for the spectra observed (Figs. 2–8), the  $g$  factor is 2.0.

Finally, in cryocrystals of the light noble gases, particularly neon, relaxation in the vibrational levels of an excimer molecule takes place very slowly, and radiation takes place

from very highly excited vibrational states, i.e., practically from free  ${}^3P_2$  atoms.

Thus, it is most probable that the short-lived centers responsible for the observed ESR spectra are the  ${}^3P_2$  atoms of these gases, localized in the noble-gas cryocrystals and interacting with the nearest environment of the cryocrystal lattice distorted by them.

## 5. CONCLUSION

In summarizing, we note the following.

An entirely new method used in this work for obtaining excited states of solid noble gases consists in directly introducing excited metastable atoms of this gas into the growing noble-gas cryocrystal, then observing the nature of the excitation of the crystal. In all the studies known thus far, excitation of the noble-gas crystals was done by a fundamentally different method, i.e., the already formed cryocrystals were irradiated by charged particles (electrons or ions) or by hard electromagnetic radiation. Excitons or ions are thus formed in the cryocrystal; this can subsequently yield to autolocalization of excitons and recombination of ions with formation of atomic or molecular local excitations accompanied by relaxation of the crystal lattice, and ends in radiation of these local centers. When an excited metastable atom is introduced into a noble-gas cryocrystal, the processes, as has been shown in this work, develop differently; apparently, the nearest crystalline environment of the atom in the growing crystal appreciably differs at once from the regular crystal lattice.

Furthermore, this work deals for the first time with the magnetic properties of excited states in noble-gas cryocrystals. We have detected and studied such interesting processes as the splitting of levels and freezing-out of the orbital angular momentum of a matrix-isolated autolocalized metastable noble-gas atom by the anisotropic electric field of the noble-gas cryocrystal lattice deformed by this atom.

In these studies, as effective a method as ESR has been used for the first time to detect and investigate excited states, and this has made it possible to obtain the new results mentioned above. All previous studies of excited states in noble-gas cryocrystals involved the use of optical methods.

The technique developed here and the results obtained with it offer essentially new possibilities in the study of excited states in cryogenic crystals.

<sup>1</sup> H. Coufal, E. Lusher, H. Micklitz, and R. E. Norberg, *Rare Gas Solids*. Berlin–Heidelberg–New York–Tokyo: Springer-Verlag, 1984 (Springer Tracts in Modern Physics 103), p. 33.

<sup>2</sup> R. A. Zhitnikov and Yu. A. Dmitriev, *Zh. Eksp. Teor. Fiz.* **92**, 1913 (1987) [*Sov. Phys. JETP* **65**, 1075 (1987)].

<sup>3</sup> Yu. A. Dmitriev and R. A. Zhitnikov, *Zh. Tekh. Fiz.* **57**, 1811 (1987) [*Sov. Phys. Tech. Phys.* **32**, 1082 (1987)].

<sup>4</sup> R. A. Zhitnikov and Yu. A. Dmitriev, *Zh. Tekh. Fiz.* **60**, 154 (1990) [*Sov. Phys. Tech. Phys.* **35**, 227 (1990)].

<sup>5</sup> R. A. Zhitnikov, Yu. A. Dmitriev, and M. E. Kaimakov, *Fiz. Nizk. Temp.* **15**, 651 (1989) [*Sov. J. Low Temp. Phys.* **15**, 367 (1989)].

<sup>6</sup> A. A. Radzig and B. M. Smirnov, *Reference Data on Atoms, Molecules, and Ions*, Springer, New York, 1985.

<sup>7</sup> T. Suemoto and H. Kanzaki, *J. Phys. Soc. Jpn.* **46**, 1554 (1979).

<sup>8</sup> J. E. Wertz and J. R. Bolton, *Electron Spin Resonance: Elementary Theory and Practical Applications*, McGraw-Hill, New York, 1972.

<sup>9</sup> A. M. Ratner and I. Ya. Fugol', *Fiz. Nizk. Temp.* **13**, 165 (1987) [*Sov. J. Low Temp. Phys.* **13**, 90 (1987)].

<sup>10</sup> O. N. Grigorashchenko, Yu. I. Rybalko, E. V. Savchenko, and I. Ya.

Fugol', *Fiz. Nizk. Temp.* **8**, 886 (1982) [*Sov. J. Low Temp. Phys.* **8**, 447 (1982)].

<sup>11</sup>E. V. Savchenko, Yu. I. Rybalko, and I. Ya. Fugol', *Pis'ma Zh. Eksp. Teor. Fiz.* **42**, 210 (1985) [*JETP Lett.* **42**, 260 (1985)].

<sup>12</sup>P. A. Braun and A. A. Kiselev, *Introduction to the Theory of Molecular Spectra* (LGU, Leningrad, 1983), p. 75.

Translated by Adam Peiperl